

Synthesis and Photophysical Studies of Thiadiazole[3,4-*c*]pyridine Copolymer Based Organic Field-Effect Transistors

Chinna Bathula^{1,2} · Sang Kyu Lee³ · Pranav Kalode⁴ · Sachin Badgujar³ · Ningaraddi S. Belavagi⁵ · Imtiyaz Ahmed M. Khazi⁵ · Youngjong Kang^{1,2}

Received: 5 November 2015 / Accepted: 27 March 2016
© Springer Science+Business Media New York 2016

Abstract A novel thiadiazolo[3,4-*c*]pyridine] based donor-acceptor (**D-A**) copolymer, poly[4,8-bis(triisopropylsilylethynyl)benzo[1,2-*b*:4,5-*b'*]dithiophene-2,6-diyl-*alt*-[4,7-bis(4-(2-ethylhexyl)thiophen-2-yl)-[1,2,5]thiadiazolo[3,4-*c*]pyridine] (**PTBDTPT**), containing triisopropylsilylethynyl(TIPS)benzo[1,2-*b*:4,5-*b'*]dithiophene as a donor is synthesized by Stille polymerization reaction. All the important photo physical prerequisites for organic field-effect transistor (OFET) application such as strong and broad optical absorption, thermal stability, and compatible HOMO-LUMO levels can be accomplished and combined on one macromolecule. Optical band gap of the polymer was found to be 1.61 eV as calculated from its film onset absorption edge. The hole mobility of bottom gate OFET using the synthesized polymer as an active channel is found to be $1.92 \times 10^{-2} \text{ cm V}^{-1} \text{ s}^{-1}$ with the On/Off ratio of 25. The photophysical study suggests that **PTBDTPT** is promising candidate for future large area organic electronic applications.

Keywords Thiadiazolo[3,4-*c*]pyridine · Benzodithiophene · Photophysical studies · Stille reaction · Organic field-effect transistors

Introduction

Organic electronics offers attractive balance between cost and performance due to versatility in its molecular structure. Remarkable progress has been made on the solution-processed organic semiconductors to replace amorphous silicon as the active layer in bulk heterojunction(BHJ) organic photovoltaics (OPVs), organic field-effect transistors (OFETs) due to their potential applications in flexible and low-cost E-paper, smart card, radio frequency identification, and displays [1–3]. Conjugated polymer backbones containing alternating electron rich donor and electron-poor acceptor units have emerged as a popular approach in the design of low band gap materials [4]. By careful consideration of the repeating donor and acceptor units, control over the highest occupied molecular orbital (HOMO) and lowest unoccupied molecular orbital (LUMO) energy levels of these polymers is possible [5]. This facilitates the design of a variety of chromophores with optimal light absorption properties for the injection and extraction of charges in OFET devices [6–8]. Some of the highest performing polymers for organic electronic applications utilize this concept [6].

The mobility in polymeric FETs especially at ambient conditions is generally low due to the poor packing of those materials. In order to solve this problem, one of the most effective approaches is to strengthen the intermolecular interactions between the neighbouring molecules by enhancing their molecular orbital overlapping. Although the large number of high performing materials have been explored for OFETs, diketopyrrolopyrrole remains as one of the most versatile

✉ Chinna Bathula
cdbathula9@gmail.com

¹ Department of Chemistry, Research Institute for Natural Sciences, Hanyang University, Seoul 133-791, Republic of Korea

² Institute of Nanoscience and Technology, Hanyang University, Seoul 133-791, Republic of Korea

³ Energy Materials Research Center, Korea Research Institute of Chemical Technology (KRICT), 141 Gajeong-ro, Yuseong-gu, Daejeon 305-600, Republic of Korea

⁴ Department of Physics and Energy Systems Research, Ajou University, Yeongtong-gu, Suwon 443-749, Republic of Korea

⁵ CPEPA, Department of Chemistry, Karnatak University, Dharwad 580 003, India

and widely used structural motifs [9, 10]. It was found that the fused aromatic rings such as thieno[3,2-*b*]-thiophene [11] provide a clear tendency to form a large orbital overlapping area, which is useful for charge carrier transport. Additionally, development of the alternating donor-acceptor (D–A) copolymers may be another versatile way to enhance mobility [12], because these polymers can exhibit closer intermolecular π – π stacking in view of the attractive forces between the donor and acceptor units. Conjugated polymers containing 2,1,3-benzothiadiazole (BTz) based D–A type of have been explored in OFET [5]. Among the reported blocks, benzo[1,2-*b*:4,5-*b'*]dithiophene (BDT) [13–16], naphthodithiophene (NDT) [17, 18], and 4,7-dithien-2-yl-2,1,3-benzothiadiazole (DTBT) [5] have been proven to be excellent donor and acceptor units. Dithienothiadiazole [3,4-*c*]pyridine (DTPT) offers a pyridyl N-atom for possible Lewis acid binding, which is more basic and accessible than the BTz counterpart [19], and makes it a stronger acceptor than BTz. The thiadiazolopyridine unit is a strong electron acceptor [20] which can lead to charge-transfer characteristics when coupled with complementary donor fragments. Copolymers incorporating the DTPT unit have been reported as effective narrow band gap materials and are shown to exhibit enhanced optoelectronic properties [21, 22].

In this research we report, a novel donor–acceptor types of conjugated polymer **PTBDTPT** based on dithienothiadiazole[3,4-*c*]pyridine acceptor and triisopropylsilylethynyl(TIPS)benzo[1,2-*b*:4,5-*b'*]dithiophene as donor for application in OFET. All the important photo physical prerequisites for organic field-effect transistor (OFET) application such as strong and broad optical absorption, thermal stability, and compatible HOMO-LUMO levels are determined in one macromolecule. Due to the presence triisopropylsilylethynyl in the donor and ethyl hexyl alkyl chain on the dithienothiadiazole[3,4-*c*]pyridine acceptor, the polymer PTBDTPT exhibited good solubility in common processing solvents for fabrication of OFET such as chloroform, chlorobenzene and O-dichlorobenzene. The hole mobility of bottom gate OFET using the polymer **PTBDTPT** as an active channel found to be $1.92 \times 10^{-2} \text{ cm V}^{-1} \text{ s}^{-1}$ with the On/Off ratio of 25. This work successfully demonstrates that dithienothiadiazole [3,4-*c*]pyridine and triisopropylsilylethynyl(TIPS)benzo[1,2-*b*:4,5-*b'*]dithiophene are promising units to build D-A copolymer for future large area organic electronics.

Experimental

Materials

Triisopropylsilyl acetylene, N,N,N,N-tetramethyl-ethane-1,2-diamine (TMEDA), trimethyltinchloride, dimethylformamide

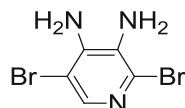
(DMF), tetrakis(triphenylphosphine)palladium, tributyl(4-(2-ethylhexyl)thiophen-2-yl)stannane, N-bromosuccinimide, bis(triphenylphosphine)palladium(II) dichloride and toluene (99.8 %, anhydrous) were purchased from Aldrich. 3, 4-diaminopyridine was Purchased from TCI. All chemicals were used without further purification. The monomers 2,6-Bis(trimethyltin)-4,8-bis(triisopropylsilylethynyl)-benzo[1,2-*b*:4,5-*b'*]dithiophene [12] and 4,7-Bis(5-bromo-4-(2-ethylhexyl)thiophen-2-yl)-[1,2,5]thiadiazolo [3,4-*c*]pyridine [19] were prepared by previously described methods.

Material Characterization

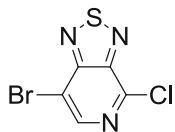
The synthesized compounds were characterized with ^1H NMR and ^{13}C NMR spectra obtained using a Bruker DPX-300 NMR spectrometer. UV-visible analysis was performed using a Lambda 20 (Perkin Elmer) diode array spectrophotometer. The number and average molecular weights of the polymers were determined by gel permeation chromatography (GPC; Viscotek) equipped with a TDA 302 detector and a PL-gel (Varian) column, using chloroform as the eluent and polystyrene as the standard. Cyclic voltammetry experiment is carried out using Weis-500 work station. Thermogravimetric analysis (TGA) was performed under a nitrogen atmosphere at a heating rate of $10 \text{ }^\circ\text{C min}^{-1}$ with a Dupont 9900 analyzer.

Synthesis of Monomer and Polymer

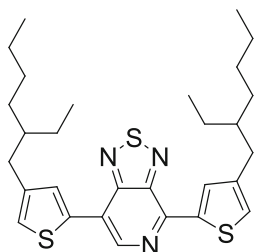
Synthesis of 2,5-dibromo-3,4-diaminopyridine (**2**).



In a three-neck 100 mL round-bottom flask, was added 3,4-diaminopyridine (**1**) (5.0 g, 45.2 mmol) with 9.3 mL of 48 % hydrobromic acid. The resulting mixture was heated to reflux while stirring and bromine (7.6 mL, 148.5 mmol) was added dropwise. The reaction mixture was refluxed for 5 h and cooled to ambient temperature. The mixture was filtered and washed with a saturated solution of $\text{Na}_2\text{S}_2\text{O}_3$ (100 mL), Na_2CO_3 (100 mL) and finally water (100 mL). To complete the neutralization process, the crude product was refluxed 30 min in a 10 % solution of Na_2CO_3 . The mixture was then filtered and washed with water. The brown-dark product was first purified by column chromatography ethyl acetate/hexane (3:2) and by recrystallization from methanol to give compound **2** as an orange powder (3.1 g, 25.5 %). ^1H NMR (Acetone- d_6 , 300 MHz, δ /ppm): 7.65 (s, 1H), 5.54 (br, 2H), 4.66 (br, 2H). ^{13}C NMR (100 MHz, Acetone- d_6 , δ /ppm): 140.66, 140.45, 129.81, 128.30, 106.24. EI-MS m/z : $[\text{M} + \text{H}]^+$ Cacl_d for $\text{C}_5\text{H}_5\text{Br}_2\text{N}_3$: 264.88, Found: 264.70.

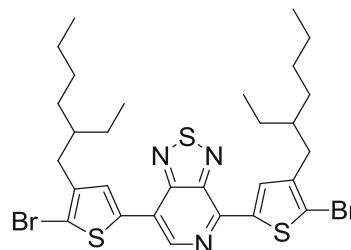
7-bromo-4-chloro [1,2,5]thiadiazolo[3,4-*c*]pyridine (**3**).

A 250 mL flame-dried flask fitted with a condenser was charged with 2.00 g (7.5 mmol) of 2,5-dibromo-3,4-diaminopyridine (**2**) and 41.00 ml (560 mmol) of thionyl chloride. The mixture was refluxed for 5 h then cooled to room temperature. The excess of thionyl chloride was evaporated and the crude product slowly neutralized with 50 mL of saturated NaHCO₃. Once the reaction quenching was completed, 100 mL of chloroform was added and the mixture transferred to a separatory funnel. The chloroform layer was separated and the aqueous layer washed two times with chloroform. The organic layers were combined, dried with MgSO₄ and the solvent removed under reduce pressure. The crude product was recrystallized from methanol to afford compound **3** pale yellow needles as the title product (1.15 g, 62 %). ¹H NMR (300 MHz, CDCl₃, δ/ppm): 8.54 (s, 1H), ¹³C NMR (100 MHz, CDCl₃, δ/ppm): 156.30, 148.68, 145.40, 144.84, 111.11, EI-MS m/z: [M + H]⁺ Calcd for C₅HBrClN₃S: 248.87, Found: 248.62.

4,7-Bis(4-(2-ethylhexyl)thiophen-2-yl)-[1,2,5]thiadiazolo[3,4-*c*]pyridine (**4**)

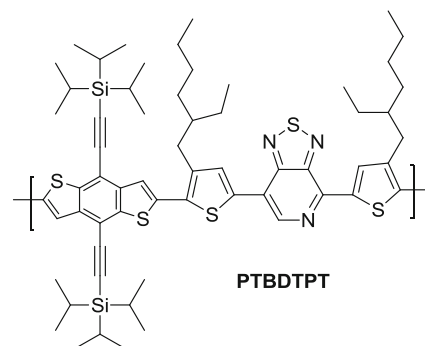
In a dry two-neck 100 mL round bottom flask, 7-bromo-4-chloro [1,2,5]thiadiazolo[3,4-*c*]pyridine (**3**) (0.50 g, 2.00 mmol), tributyl(4-(2-ethylhexyl)thiophen-2-yl)stannane (1.64 g, 4.60 mmol) and Pd(PPh₃)₂Cl₂ (0.10 g) were added under the protection of N₂. Dry THF (12 mL) and DMF (12 mL) were injected through a syringe. The reaction mixture was heated to reflux for 12 h, then the mixture was allowed to cool down to room temperature and poured into water (50 mL). The organic phase was next separated and the aqueous phase extracted by chloroform (3 X 50 mL). After removal of the solvent, the solid was purified by column chromatography on silica gel using petroleum ether/dichloromethane (10:1) as eluent to get the crude product. Further purification was carried out by recrystallization with ethanol to obtain the pure compound **4** as red crystals (0.63 g, 70 %), ¹H NMR (CDCl₃, 300 MHz, δ/ppm): 8.81 (s, 1H), 8.50 (s, 1H), 7.93 (s, 1H), 7.18

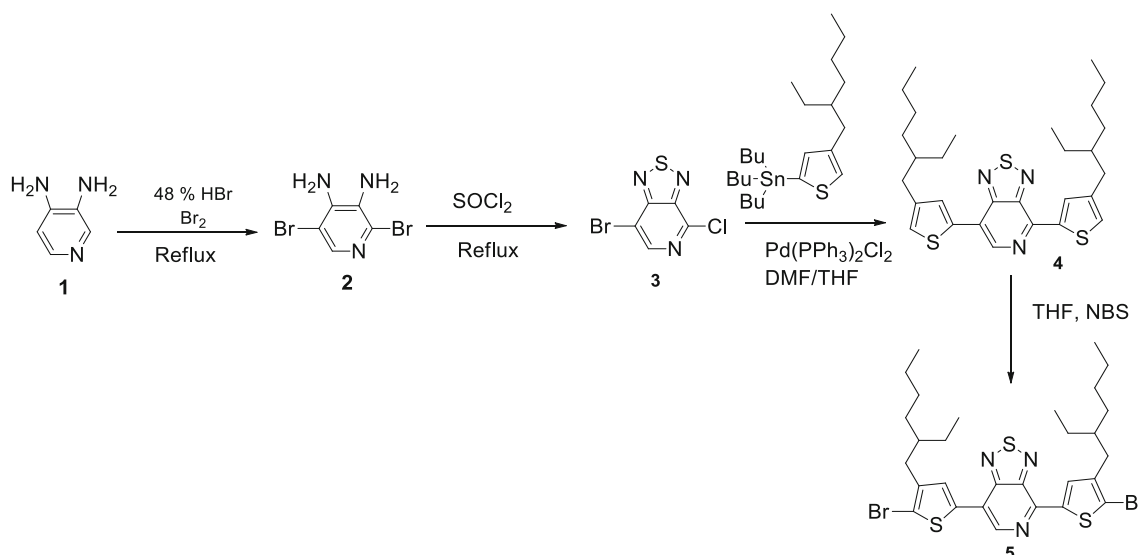
(s, 1H), 7.05 (s, 1H), 2.64 (t, 4H), 1.66 (m, 2H), 1.21–1.42 (m, 16H), 0.95 (m, 12H). ¹³C NMR (CDCl₃, 100 MHz, δ/ppm): 155.06, 148.18, 146.46, 144.12, 143.34, 141.28, 140.76, 136.15, 133.70, 129.93, 126.68, 120.30, 120.63, 40.46, 34.71, 32.60, 29.03, 25.77, 23.23, 14.33, 11.02. EI-MS m/z: [M + H]⁺ Calcd for C₂₉H₃₉N₃S₃: 525.84, Found: 525.23.

4,7-Bis(5-bromo-4-(2-ethylhexyl)thiophen-2-yl)-[1,2,5]thiadiazolo[3,4-*c*]pyridine (**5**)

In a dry two-neck 50 mL round bottom flask, 4,7-Bis(4-(2-ethylhexyl)thiophen-2-yl)-[1,2,5]thiadiazolo[3,4-*c*]pyridine (**4**) (0.50 g, 0.95 mmol) was dissolved in dry THF (20 mL) at room temperature. Then the reaction mixture was stirred in an ice bath for 15 min, NBS (0.440 g, 2.35 mmol) was added in small portions in dark. After stirring for about 10 h, the reaction mixture was washed with water (100 mL), and the organic layer was dried over anhydrous Na₂SO₄. The solvent was removed to give the product as a red solid. The solid was purified by column chromatography on silica gel using petroleum ether/dichloromethane (10:1) as eluent to get the crude product. Further purification was carried out by recrystallization with ethanol to obtain the pure compound **5** as red crystals (0.430 g, 67 %). ¹H NMR (CDCl₃, 300 MHz, δ/ppm): 8.69 (s, 1H), 8.32 (s, 1H), 7.74 (s, 1H), 2.58 (t, 4H), 1.71 (m, 2H), 1.20–1.40 (m, 16H), 0.91 (m, 12H). ¹³C NMR (CDCl₃, 100 MHz, δ/ppm): 154.66, 147.80, 145.52, 143.58, 142.68, 140.86, 140.19, 135.82, 133.24, 129.15, 119.95, 117.22, 112.62, 40.10, 34.16, 32.60, 28.91, 25.84, 23.23, 14.32, 11.02. EI-MS m/z: [M + H]⁺ Calcd for C₂₉H₃₇Br₂N₃S₃: 683.64, Found: 683.40.

Synthesis of poly[4,8-bis(triisopropylsilyl)ethynyl]benzo[1,2-*b*:4,5-*b'*]dithiophene-2,6-diyl-*alt*-[4,7-bis(4-(2-ethylhexyl)thiophen-2-yl)-[1,2,5]thiadiazolo[3,4-*c*]pyridine] (**PTBDTPT**).

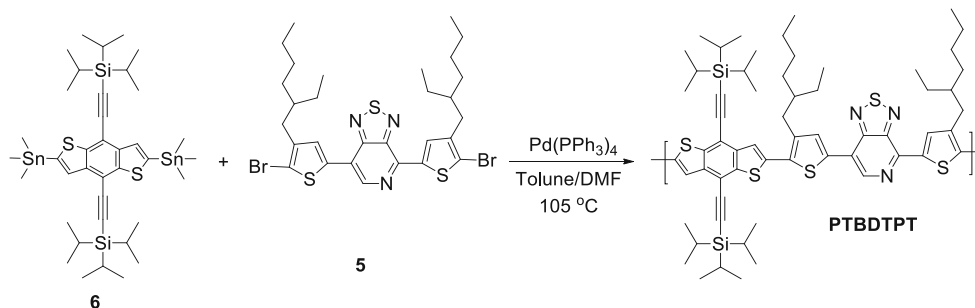




Scheme 1 Synthetic route for DTPT monomer

2,6-Bis(trimethyltin)-4,8-bis(triisopropylsilyl)ethynylbenzo[1,2-b:4,5-b']dithiophene (**6**) (262 mg, 0.3 mmol), 4,7-Bis(5-bromo-4-(2-ethylhexyl)thiophen-2-yl)-[1,2,5]thiadiazolo[3,4-*c*]pyridine (**5**) (205 mg, 0.3 mmol) and Pd(PPh₃)₄ (14 mg, 0.05 eq.) were added to a 50 mL round-bottom flask. Then, anhydrous DMF (1 mL) and anhydrous toluene (4 mL) were added. The polymerization was carried out at 105 °C under argon protection. Then, anhydrous DMF (1 mL) and anhydrous toluene (4 mL) were added. The polymerization was carried out at 105 °C under argon protection. After 24 h, the reaction mixture was cooled to about 50 °C and added slowly to a vigorously stirred methanol (50 mL). The polymer fibers were collected by filtration. The polymer was dissolved in chlorobenzene and precipitated again into methanol. The precipitate was then subjected to Soxhlet extraction with methanol, acetone, hexanes, and chloroform. The final polymer is obtained by evaporation of chloroform and precipitating in methanol. The polymer is filtered and dried in vacuo at 40 °C for 12 h. Dark blue shining material is obtained in the yield of 73 %. ¹H NMR (CDCl₃, 300 MHz, δ/ppm): 8.64 (br, 1H), 8.26 (br, 1H), 7.58 (br, 2H), 7.62 (br, 1H), 2.47 (br, 4H), 1.68 (br, 2H), 1.20–1.40 (br, 58H), 0.93 (br, 12H). Anal. calcd: C, 68.31; H, 7.95; N, 3.81, S, 14.54; found C, 68.20; H, 7.86; N, 3.72, S, 14.48.

Scheme 2 Synthetic route for PTBDTPT copolymer



Results and Discussion

Synthesis and Characterization of the Monomer and Polymer

The acceptor monomer 4,7-Bis(5-bromo-4-(2-ethylhexyl)thiophen-2-yl)-[1,2,5]thiadiazolo[3,4-*c*]pyridine was synthesized as depicted in (Scheme 1). First step involves bromination of 3,4-diaminopyridine with 48 % hydrobromic acid resulting in the formation of 2,5-dibromo-3,4-diaminopyridine (**2**). Thus obtained intermediate is subjected for ring closure reaction using thionyl chloride to obtain 7-bromo-4-chloro [1,2,5]thiadiazolo[3,4-*c*]pyridine (**3**). The next step consisted of palladium catalyzed Stille reaction of compound (**3**) and tributyl(4-(2-ethylhexyl)thiophen-2-yl)stannane leading to an intermediate 4,7-Bis(4-(2-ethylhexyl)thiophen-2-yl)-[1,2,5]thiadiazolo[3,4-*c*]pyridine (**4**), followed by bromination using NBS to accomplish the synthesis of monomer 4,7-Bis(5-bromo-4-(2-ethylhexyl)thiophen-2-yl)-[1,2,5]thiadiazolo[3,4-*c*]pyridine (**5**). The thiadiazolo [3,4-*c*]pyridine based co-polymer **PTBDTPT** is synthesized by polycondensation of 2,6-bis(trimethyltin)-4,8-bis(triisopropylsilyl)ethynyl-benzo[1,2-b:4,5-b']dithiophene (**6**) and 4,7-Bis(5-bromo-4-(2-

ethylhexyl)thiophen-2-yl)-[1,2,5]thiadiazolo[3,4-*c*]pyridine (5) through the palladium catalyzed Stille reaction (Scheme 2). The crude polymers were extracted with chloroform and precipitated in methanol followed by washing with methanol and acetone, successively, via Soxhlet apparatus to remove by-products and oligomers. The final polymers were obtained by evaporation of chloroform and precipitating in methanol. The number average molecular weights (M_n) were determined by gel permeation chromatography (GPC) against polystyrene standards in a chloroform eluent (Table 1). M_n of the polymer is found to be 12.9 kg mol^{-1} with a polydispersity index of 1.93 (Table 1).

Thermal Properties

The thermal properties of copolymers were evaluated by thermogravimetric analysis (TGA) under a nitrogen atmosphere at a heating rate of $10 \text{ }^\circ\text{C min}^{-1}$ (Fig. 1). The polymer exhibited good thermal stability, showing a weight loss of less than 5 % at temperature up to $350 \text{ }^\circ\text{C}$ indicating sufficient thermal stability for OFET applications. The physical properties of the polymer are summarized in (Table 1).

Optical Properties

The optical properties of the polymer are obtained by UV-Vis with chloroform solution and thin film are shown in Fig. 2. The absorption bands of PTBDTPT for solution were observed at 350 nm, 430 nm and 620 nm while those of film were seen at 360 nm, 450 nm and 650 nm. The higher energy absorbances were attributed to localized π - π^* transitions while the lower energy bands were associated with an intramolecular charge transfer (ICT) between the donor and acceptor similar to those characterized for by Jespersen et al. [23, 24]. The optical properties of the polymer film are slightly red-shifted by 30 nm most likely due to high co-planarity and/or enhanced intermolecular electronic interactions in the solid state such that lead to stability of a lower energy excited state. The optical band gap obtained by extrapolating the absorption edge of the film is 1.61 eV. These results support that the polymer showed low band gap. The optical properties are summarized in Table 2.

Table 1 Physical properties of the polymer

Polymer	M_n^a [kg/mol]	M_w^a [kg/mol]	PDI	Yield [%]	T_d^b [$^\circ\text{C}$]
PTBDTPT	12.9	25.3	1.93	73	350

^a The molecular weights were determined by using gel permeation chromatography (GPC) against polystyrene standards in chloroform eluent,

^b Temperature resulting in 5 % weight loss based on initial weight

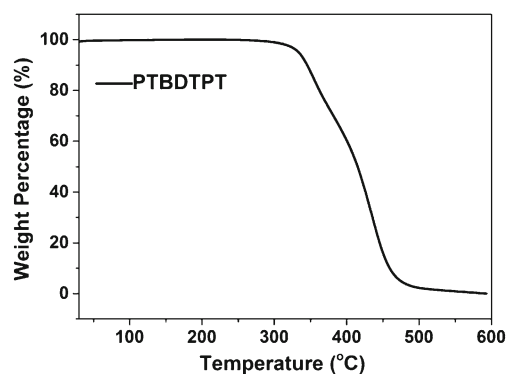


Fig. 1 TGA plots for the polymer, obtained with a heating rate of $10 \text{ }^\circ\text{C min}^{-1}$ under an inert atmosphere

Electrochemical Properties

We studied the electrochemical properties of the polymer by cyclic voltammetry in order to estimate their HOMO and LUMO energy levels. The onset oxidation and reduction potentials obtained are correspond to the HOMO and LUMO energy levels, respectively. The electrochemical properties of polymer as thin film on a platinum electrode in 0.1 M Bu_4NPF_6 acetonitrile solution at a scan rate of 50 mV s^{-1} are determined. As seen in Fig. 3, the onset oxidation potential of PTBDTPT is found to be at 0.50 eV versus Ag/AgCl respectively. Using ferrocene as a reference value with -4.8 eV below the vacuum level [21], the HOMO energy levels of the polymers approximating using Eq. (1),

$$E_{\text{HOMO}} = -(E_{\text{OX}} - E_{\text{Fc}} + 4.8)(\text{eV}) \quad (1)$$

wherein E_{Fc} is the potential of the internal standard, the ferrocene/ferrocenium ion (Fc/Fc^+) couple. The value of E_{Fc} , which is determined under the same experimental conditions is approximately 0.25 eV vs Ag/Ag^+ .

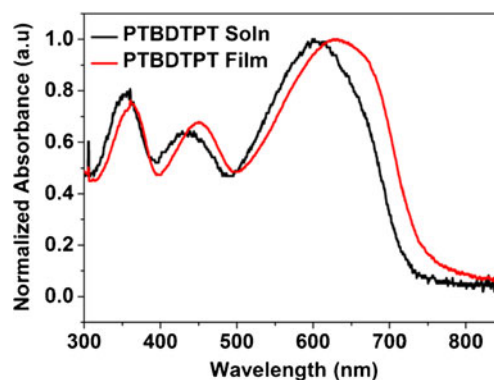


Fig. 2 UV-Vis absorption spectra of the polymer in chloroform solution and thin film

Table 2 Optical and electrochemical properties of the polymer

Polymer	$\lambda_{\max}^{\text{abs,Sol}}$ ^a [nm]	$\lambda_{\max}^{\text{abs,Film}}$ ^a [nm]	HOMO ^b [eV]	LUMO ^c [eV]	E_g^{opt} ^d [eV]
PTBDTPT	620	650	-5.15	-3.54	1.61

^a The UV-Vis absorption spectra of the polymers were measured in chloroform solution and thin film,

^b HOMO levels of the polymer were determined from onset voltage of the first oxidation potential with reference to ferrocene at -4.8 eV,

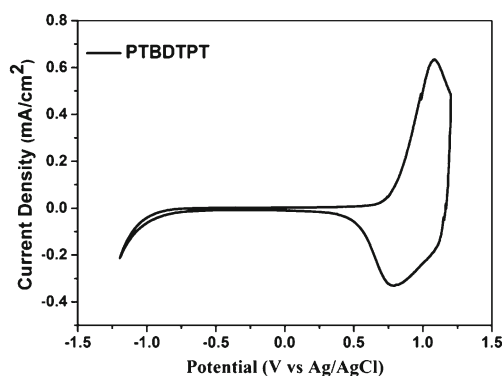
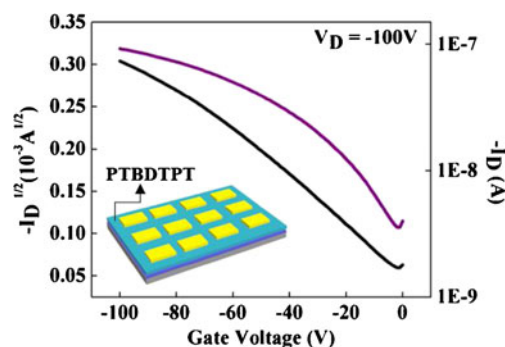
^c LUMO levels of the polymer were estimated from the optical band gaps and the HOMO energy levels,

^d Optical band gap was calculated from the UV-Vis absorption onset in film

The HOMO energy levels of the polymer is found to be -5.15 eV. From this value, the LUMO energy levels of the polymer is obtained using Eq. (2)

$$E_{\text{LUMO}} = E_{\text{HOMO}} + E_g^{\text{opt}} \text{ (eV)} \quad (2)$$

The LUMO values are determined to be -3.54 eV such that the energy gap between the HOMO and LUMO to be 1.61 eV. The electrochemical properties are summarized in Table 2. These data are determined by UV-visible and cyclic voltammetry (CV) experiments show that the presence of the strong acceptor in the polymer resulted in a lower energy HOMO as well as LUMO while maintaining a lower overall band gap. Cyclic voltammetry is used in order to estimate HOMO and LUMO energy levels and UV visible test is performed to determine optical band gap (E_g^{opt}) of the polymer material. By careful consideration of the repeating donor and acceptor units, control over the highest occupied molecular orbital (HOMO) and lowest unoccupied molecular orbital (LUMO) energy levels of these polymers is possible. This facilitates the optimal light absorption properties for the injection and extraction of charges in OFET devices.

**Fig. 3** Cyclic Voltammogram of the thin film of the polymer**Fig. 4** Transfer characteristics of OFET fabricated with Polymer PTBDTPT at $V_D = -100$ V. Inset shows a schematic of FET structure used in this study

Organic Field Effect Transistors (OFET)

The effects of the donor segment on the electrical transport properties of the resulting materials were examined by fabricating OFET. Figure 4 illustrates typical transfer and output characteristics of OFET using PTBDTPT as an active channel. Inset shows a schematic of OFET device used in this study. Top contact bottom gate FETs were fabricated on silicon (Si) wafer covered with 300 nm silicon oxide (SiO_2). Samples were first cleaned with Piranha solution for 20 min at 80 °C followed by carefully rinsing with distilled water, ethanol and finally blown dry with a stream of nitrogen gas. Then SiO_2/Si samples were treated with UV ozone for 2 min to make its surface hydrophilic. The PTBDTPT polymer layer in chlorobenzene solution was spin-coated on UV ozone treated SiO_2/Si substrate with concentration of 5 mg mL⁻¹ at 3000 RPM for 30s. Samples were further dried at 80 °C for 10 min on hot plate to remove residual solvents. 50 nm thick Au electrodes were deposited as source and drain through metal shadow mask (channel length (L) = 50 μm and width (W) = 100 μm) in thermal evaporator. All the electrical characterizations were performed in dark under ambient air using semiconductor parameter analyzer Agilent 4155C. The hole mobility of polymer in the saturation region [18] was calculated using following equation,

$$I_{ds} = (WC_i/2L)\mu(V_G - V_T)^2 \quad (3)$$

where I_{ds} is the drain-source current in the saturated region, W and L are the channel width and length, respectively, μ is the field-effect mobility, C_i is the capacitance per unit area of the

Table 3 Device characteristics of solution processed OFET

Polymer	μ_{\max} [cm ² V ⁻¹ s ⁻¹]	^a $I_{\text{on}}/I_{\text{off}}$
PTBDTPT	1.92×10^{-2}	25

^a $I_{\text{on}}/I_{\text{off}}$ refers to the corresponding on-to-off ratio and the threshold voltage at the maximum hole mobility

insulation layer (SiO_2 , 300 nm), and V_G and V_T are the gate and threshold voltages, respectively.

The bottom gate field effect mobility of polymer **PTBDTPT** in saturation region was found to be $1.92 \times 10^{-2} \text{ cm}^2 \text{ V}^{-1} \text{ S}^{-1}$ with ON/OFF ratio more than 25 and Drain voltage $V_D = -100 \text{ V}$. The OFET devices made using the polymer **PTBDTPT** exhibited typical p-type characteristics. Results are summarized in Table 3. These results clearly demonstrate that both the backbone and side chains of the polymers have a great influence on the corresponding OFET performance. The enhanced electrical properties can be also attributed to the coplanarity of **PTBDTPT** polymer that results into layer by layer self-assembly during spin coating process. This ultimately results in improving on current which evidently improves mobility and On/Off ratio. Further studies are currently underway to gain better understanding of charge transport mechanism.

Conclusions

In summary, the present work successfully demonstrated the synthesis and characterization of novel donor–acceptor type of conjugated polymer (**PTBDTPT**) based on the dithienothiadiazole[3,4-*c*]pyridine and triisopropylsilylethynyl(TIPS)benzo[1,2-*b*:4,5-*b'*]dithiophene units, for application in OFET. The hole mobility of bottom gate OFET using the polymer as an active channel found to be $1.92 \times 10^{-2} \text{ cm}^2 \text{ V}^{-1} \text{ S}^{-1}$ with the On/Off ratio just over 25, at room temperature in ambient conditions. Photophysical studies suggest the polymer to be promising candidate for organic electronics. Additional modifications to the polymer structure and device are currently under study to further improve the OFET performance.

Acknowledgments We gratefully acknowledge the support by Samsung Research Funding Center of Samsung Electronics under Project Number SRFC-MA1401-05.

References

1. Heeger AJ (2001) Semiconducting and Metallic polymers: the Fourth Generation of polymeric Materials. *Angew Chem Int Ed* 40:2591–2611
2. Lewis NS (2007) Toward Cost-Effective Solar energy use. *Science* 315:798–801
3. Bijleveld JC, Zoombelt AP, Mathijssen SG, Wienk MM, Turbiez M, de Leeuw DM, Janssen RA (2009) Poly(diketopyrrolopyrrole-terthiophene) for Ambipolar Logic and Photovoltaics. *J Am Chem Soc* 131:16616–16617
4. Yu G, Gao J, Hummelen JC, Wudl F, Heeger AJ (1995) Polymer Photovoltaic cells: Enhanced Efficiencies via a Network of Internal Donor-Acceptor Heterojunctions. *Science* 270:1789–1791
5. Park SH, Roy A, Beaupre S, Cho S, Coates N, Moon JS, Moses D, Leclerc M, Lee K, Heeger AJ (2009) Bulk heterojunction solar cells with internal quantum efficiency approaching 100 %. *Nature Photonics*. 3:297–302
6. Alan H (2014) 25th Anniversary Article: bulk heterojunction Solar cells: Understanding the Mechanism of Operation. *Adv Mater* 26: 10–28
7. Coffin R, Peet J, Rogers J, Bazan G (2009) Streamlined microwave-assisted preparation of narrow-bandgap conjugated polymers for high-performance bulk heterojunction solar cells. *Nat Chem* 1:657–661
8. Kang I, Yun D, Chung S, Kwon S, Kim Y (2013) Record high hole mobility in polymer semiconductors via Side-Chain Engineering. *J Am Chem Soc* 135:14896–14899
9. Bathula C, Sachin B, Belavagi NS, Lee SK, Kang Y, Khazi IM (2016) Synthesis, characterization and optoelectronic properties of benzodithiophene Based copolymers for Application in Solar cells. *J Fluoresc* 26:371–376
10. Kim J-H, Lee M, Yang H, Hwang D-H (2014) High molecular weight triisopropylsilylethynyl (TIPS)-benzodithiophene and Diketopyrrolopyrrole-Based copolymer for high performance organic photovoltaic cells. *J Mater Chem A* 2:6348–6352
11. Yuning L, Samarendra S, Prashant S (2010) A high mobility p-type DPP-Thieno[3,2-*b*]thiophene copolymer for Organic Thin-Film Transistors. *Adv. Mate* 22:4862–4866
12. Bathula C, Song CE, Sachin B, Hong S-J, Kang I-N, Moon S-J, Lee J, Cho S, Shim H-K, Lee V (2012) New TIPS-substituted benzo[1,2-*b*:4,5-*b'*]dithiophene-based copolymers for application in polymer solar cells. *J Mater Chem* 22:22224–22232
13. Liang Y, Xu Z, Xia J, Tsai S-T, Wu Y, Li G, Ray C, Yu L (2010) For the Bright Future-Bulk heterojunction polymer Solar cells with Power Conversion efficiency of 7.4 %. *Adv Mater* 22:E135–E138
14. Zhou HX, Yang LQ, Stuart AC, Price SC, Liu SB, You W (2011) Development of Fluorinated Benzothiadiazole as a Structural unit for a polymer Solar Cell of 7 % efficiency. *Angew Chem Int Ed* 50: 2995–2998
15. Price SC, Stuart AC, Yang L, Zhou H, You W (2011) Fluorine substituted Conjugated polymer of medium band gap yields 7 % efficiency in polymer – fullerene solar cells. *J Am Chem Soc* 133: 4625–4631
16. Bathula C, Kim M, Song CE, Shin WS, Hwang D-H, Lee J-C, Kang I-N, Lee SK, Park T (2015) Concentration-dependent pyrene-driven self-assembly in benzo[1,2-*b*:4,5-*b'*]dithiophene(BDT) Thienothiophene(TT) – Pyrene copolymers. *Macromolecules* 48: 3509–3515
17. Sanjaykumar SR, Badgujar S, Song CE, Shin WS, Moon S-J, Kang I-N, Lee J, Cho S, Lee SK, Lee J-C (2012) Synthesis and characterization of a novel naphthodithiophene-based copolymer for use in polymer solar cells. *Macromolecules* 45:6938–6945
18. Bathula C, Song CE, Sachin B, Hong S-J, Park S-J, Shin WS, Lee J-C, Cho S, Ahn T, Cho S, Moon S-J, Lee SK (2013) Naphtho[1,2-*b*:5,6-*b'*]dithiophene-based copolymers for applications to polymer solar cells. *Polym Chem* 4:2132–2139
19. Huaxing Z, Yang L, Price SC, Knight KJ, You W (2010) A Geometric Approach to the Crystallographic solution of nonconventional DNA structures: helical superstructures of d(CGATAT). *Angew. Chem. Int. Ed.* 49:7920–7922
20. Karsten BP, Bijleveld JC, Viani L, Cornil J, Gierschner J, Janssen RA (2009) Electronic structure of small band gap oligomers based on cyclopentadithiophenes and acceptor units. *J Mater Chem* 19: 5343–5350
21. Bathula C, Kalode P, Supriya P, Lee SK, Belavagi NS, Khazi IM, Kang Y (2016) Synthesis and electronic properties of thiazole[3,4-*c*]pyridine copolymers for solar cell application. *Tetrahedron Lett.* 57:998–1002
22. Fukumoto H, Yamamoto T (2008) Preparation and chemical properties of soluble π -conjugated poly(aryleneethynylene) consisting of azabenzothiadiazole as the electron-accepting unit. *J. Polym. Sci., Part A: Polym. Chem.* 46:2975–2982

-
23. Jespersen KG, Beenken WJ, Zaushitsyn Y, Yartsev A, Andersson M, Pullerits T, Sundstrom V (2004) The electronic states of polyfluorene copolymers with alternating donor-acceptor units. *J Chem Phys* 121:12613–12617
 24. Yang H-Y, Sun Y-K, Chuang Y-Y, Wang T-L, Shieh Y-T, Chen W-J (2012) Electrochemical impedance parameters elucidate performance of carbazole–triphenylamine–ethylenedioxythiophene-based molecules in dye-sensitized solar cells. *Electrochim Acta*. 69:256–267